

# Supporting Information

## Prediction, Application, and Mechanism Exploration of Liquid–Liquid Equilibrium Data in the Extraction of Aromatics Using Sulfolane

Shilong Dong <sup>1</sup>, Xiaoyan Sun <sup>1,\*</sup>, Lili Wang <sup>1</sup>, Yanjing Li <sup>1</sup>, Wenyong Zhao <sup>2</sup>, Li Xia <sup>1,\*</sup> and Shuguang Xiang <sup>1</sup>

<sup>1</sup> Institute of Process System Engineering, College of Chemical Engineering, Qingdao University of Science and Technology, Qingdao 266042, China

<sup>2</sup> College of Chemistry and Chemical Engineering, Qilu Normal University, Jinan 250200, China

\* Correspondence: sxy@qust.edu.cn (X.S.); xiali@qust.edu.cn (L.X.)

### Index

S1. The detailed analysis method of water content in sulfolane.

S2. The GC performance verification method.

S3. The definition of partition coefficient ( $D$ ) and separation factor ( $S$ ).

S4. The details of LLE data predicted using the COSMO-RS method.

S5. The effect of feed situations on the extraction model.

S6. The analysis of  $\sigma$ -profiles.

S7. The interaction analysis.

S8. The calculation details of NRTL and UNIQUAC models.

**Table S1.** Chemical properties of materials.

**Table S2.** The specific test conditions for Agilent GC7890A.

**Table S3.** The test results of gas chromatograph (FID) performance verification.

**Table S4.** Liquid–liquid equilibrium data (molar fraction) for non-aromatics (1)–benzene (2)–sulfolane (3) ternary systems at 293.15 K, or 313.15 K under 101.3 kPa using the COSMO-RS model.

**Table S5.** Liquid–liquid equilibrium data (molar fraction) for non-aromatics (1)–toluene (2)–sulfolane (3) ternary systems at 293.15 K, or 313.15 K under 101.3 kPa using the COSMO-RS model.

**Table S6.** The *RMSD* values of the COSMO-RS model at 293.15 K, or 313.15 K under 101.3 kPa.

**Table S7.** Comparison of the main process indexes of C01.

**Table S8.** Interaction energy of eight complexes corrected using BSSE.

**Table S9.** The *RMSD* values of NRTL and UNIQUAC models.

**Table S10.** The binary interaction parameters for ternary mixtures using a UNIQUAC model.

**Table S11.** The feed compositions (stream 2) of the extraction device.

**Table S12.** The key components setting of C01.

**Figure S1.** The  $\sigma$ -profiles of the nine substances in this study.

**Figure S2.** The complex configurations with the lowest energies.

**Figure S3.** The RDG (left) and IGMH (right) of different complexes.

S1. The detailed analysis method of water content in sulfolane.

In this work, the water content of sulfolane was determined using an SF-3 Karl Fischer micro moisture analyzer. First of all, open the moisture analyzer. After the moisture in the moisture analyzer is completely electrolyzed and buzzes, use the micro injector to absorb sulfolane 20  $\mu\text{L}$  and inject into the moisture analyzer. The sample mass of sulfolane was measured using the decrement method after electrolysis was completed and the measured value was recorded. The sulfolane sample was determined three times, and the average value was taken as the experimental data. The equation for the water content in sulfolane is as follows:

$$X_{\text{sulfolane}} = \frac{m_1 \times 10^{-6}}{m_2} \times 100\%$$

where  $m_1$  denotes the measured value ( $\mu\text{g}$ ) of moisture in sulfolane,  $m_2$  denotes the injected mass value (g) of sulfolane, and  $X_{\text{sulfolane}}$  represents the water content (mass fraction) in sulfolane.

## S2. The GC performance verification method.

To verify the accuracy of chromatographic method according to the technical indicators established by the Chinese calibration protocol, the test was carried out according to the method. In this work, the performance verification method of GC with FID as detector is as follows:

### (1) Main instruments and chemicals

Stopwatch, division value 0.01s; microinjector, range 10  $\mu\text{L}$ ; platinum resistance thermometer, Pt100, error  $\pm 0.3$  K; digital multimeter; *n*-hexadecane/isooctane standard solution for GC verification, 100  $\mu\text{g}\cdot\text{ml}^{-1}$ , purchased from Aladdin.

### (2) Environmental conditions and detector system test conditions

Room temperature,  $294.15 \pm 0.5$  K (requirement range is 278.15 to 308.15 K); indoor relative humidity,  $53 \pm 0.5$  % (requirement range is 20 to 80 %). The detector system test conditions are shown in Table S2.

### (3) Temperature accuracy of column chamber

The platinum resistance thermometer cable was connected to the digital multimeter and the thermometer probe was fixed in the middle of the column chamber. Then, the column chamber was set to 343.15 K and heated up. After the temperature of the column chamber stabilized, we observed it for 10 minutes and the temperature of the column chamber was recorded once for each change of number. The temperature difference between maximum value and minimum value of the digital multimeter was calculated, and the ratio of the difference to the arithmetic mean of temperature measurements within 10 minutes is the temperature accuracy of the column chamber.

### (4) Programmed temperature repeatability

Based on the verification conditions and methods in Section (3), the programmed temperature repeatability test was carried out. The initial temperature was set at 323.15 K and the end temperature was 473.15 K. The temperature was increased to 473.15 K at a rate of 10  $\text{K}\cdot\text{min}^{-1}$ . After the initial temperature was stabilized, the temperature increase started, and the data was recorded every minute until the final temperature was stabilized. This process was repeated three times. The maximum relative deviation of the corresponding point was calculated according to the following equation:

$$\text{relative deviation} = \frac{t_{\max} - t_{\min}}{\bar{t}} \times 100\%$$

Here,  $t_{\max}$  and  $t_{\min}$  denote the maximum and minimum temperature (K) of the corresponding point, respectively;  $\bar{t}$  represents the average temperature (K) of the corresponding point.

#### (5) Baseline noise and baseline drift

The parameters of the gas chromatograph were set, and the baseline was recorded for at least 30 minutes after the instrument was stabilized. The 5 minutes with large noise of the recorded baseline was selected as the baseline for noise calculation. We drew parallel envelopes with 1 minute as the boundary, and measured the distance between the two parallel lines directly to the time axis. The baseline noise was calculated according to the following equation:

$$N_d = \sum_{i=1}^5 y_i / n$$

Here,  $N_d$  denotes baseline noise (A);  $y_i$  represents the baseline width of the  $i$ 'th parallel envelope (A); and  $n$  indicates the number of parallel envelopes ( $n = 5$ ). The baseline drift was recorded for 30 minutes of continuous operation, which is the average slope of the noise envelope.

#### (6) Limit of detection

The parameters of the gas chromatograph were set and we waited for the instrument to stabilize. The sample was injected 1  $\mu$ L and measured seven times. The peak area of  $n$ -hexadecane was calculated using gas chromatography and the arithmetic mean of the seven peak areas was obtained. The limit of detection was calculated according to the following equation:

$$D_{\text{FID}} = \frac{2NW}{A}$$

where  $D_{\text{FID}}$  represents the limit of detection ( $\text{g}\cdot\text{s}^{-1}$ ) of FID;  $N$  denotes the baseline noise (A);  $W$  indicates the  $n$ -hexadecane injection volume (g); and  $A$  indicates the arithmetic mean of the peak areas of  $n$ -hexadecane ( $\text{A}\cdot\text{s}^{-1}$ ).

#### (7) Quantitative repeatability

The relative standard deviation of solute retention time for seven consecutive injections was the qualitative repeatability. The quantitative repeatability was calculated according to the following equation:

$$RSD_{\text{Quantitative repeatability}} = \sqrt{\frac{\sum_{i=1}^n (t_i - \bar{t})^2}{n-1}} \times \frac{1}{\bar{t}} \times 100\%$$

Here,  $RSD_{\text{Quantitative repeatability}}$  represents the relative standard deviation;  $n$  and  $i$  represent the measurement times and injection serial number, respectively;  $t_i$  denotes the retention time of the  $i$ 'th measurement; and  $\bar{t}$  indicates the arithmetic mean value of retention time for  $n$  samples.

#### (8) Qualitative repeatability

The relative standard deviation of solute peak area for seven consecutive injections was the qualitative repeatability. The qualitative repeatability was calculated according to the following equation:

$$RSD_{\text{Qualitative repeatability}} = \sqrt{\frac{\sum_{i=1}^n (A_i - \bar{A})^2}{n-1}} \times \frac{1}{\bar{A}} \times 100\%$$

Here,  $A_i$  denotes the peak area of the  $i$ 'th measurement and  $\bar{A}$  represents the arithmetic mean value of peak area for  $n$  samples. The other symbols are as described above.

#### (9) Linearity range

The concentration of five points was chosen in the linear range evenly. The sample was injected 1  $\mu\text{L}$  and each sample was measured three times. The arithmetic mean of the  $n$ -hexadecane peak area was calculated and made the relationship between the sample volume and the peak area. The ratio of the maximum and minimum injection volume with linear  $\gamma = 0.999$  was the linearity range.

#### (10) Results

The performance of the gas chromatograph used in this experiment was verified using the above method, and the results are shown in Table S3. The data in Table S3 shows that the performance indexes of the gas chromatograph used in this work all meet the requirements.

S3. The definition of partition coefficient ( $D$ ) and separation factor ( $S$ ).

The partition coefficient ( $D$ ) and separation factor ( $S$ ) are often used to evaluate the effectiveness of separation in liquid–liquid extraction processes [1,2].  $D$  is the ratio of the mass fraction of the extracted substance in the extract phase to that in the raffinate phase. A larger  $D$  value corresponds to a higher extraction capacity of the solvent.  $S$  reflects the ease of separation of the two substances in the liquid phase of the extraction system. The larger the  $S$  value, the higher the selectivity of the extractant for the extracted substance.

$$D = \frac{w_2^I}{w_2^{II}}$$

$$S = \frac{w_2^I w_1^{II}}{w_2^{II} w_1^I}$$

Here, the superscripts I and II represent the extract and raffinate phases, respectively.

The subscripts 1 and 2 denote non-aromatic and aromatic compounds, respectively.

1. Ma, S.; Li, J.; Li, L.; Shang, X.; Liu, S.; Xue, C.; Sun, L. Liquid-liquid extraction of benzene and cyclohexane using sulfolane-based low transition temperature mixtures as solvents: Experiments and simulation. *Energy & Fuels* **2018**, *32*, 8006–8015. <https://doi.org/10.1021/acs.energyfuels.8b01524>.
2. Li, H.; Zhang, Y.; Zhao, L.; Sun, D.; Gao, J.; Xu, C. Liquid-liquid equilibria and mechanism exploration for the extraction of sulfides from FCC naphtha via organic solvent as extractant. *J. Mol. Liq.* **2021**, *327*, 114821. <https://doi.org/10.1016/j.molliq.2020.114821>.

S4. The details of LLE data predicted using the COSMO-RS method.

The COSMO-RS model obtained the  $\sigma$ -profile using quantitative calculations, and then combined statistical thermodynamic methods to calculate the chemical potential. The affinity of each compound for the two phases was calculated from the thermodynamic equilibrium partition constants ( $K_i$ ).

$$K_i = \exp\left(\frac{\mu_i^I - \mu_i^{II}}{RT}\right)$$

where  $\mu_i^I$  and  $\mu_i^{II}$  are the chemical potentials of compound  $i$  in phase I and phase II, respectively. The process of calculating  $K_i$  may be repeated until the two phases reach thermodynamic and mass equilibrium. Finally, the mole fraction of each compound in the two phases were calculated based on their  $K_i$ .

S5. The effect of feed situations on the extraction model.

In this work, the data obtained by prediction and experimentation were used at 313.15 K under a pressure of 101.3 kPa to verify these data on the modeling. The verifying of these data was performed in the process shown in Figure 10. In this process, we kept the binary interaction key component in the C01 column unchanged except for 3-methylpentane and cyclopentane, and the parameters of 3-methylpentane and cyclopentane were changed. To begin, the parameters of 3-methylpentane and cyclopentane were missing and estimated using the UNIFAC model; the calculated data are presented in detail in Table S7. As shown in Table S7, the calculated value of benzene in the bottom of the C01 column deviates greatly from the actual industrial data. Then, the parameters of 3-methylpentane and cyclopentane were simulated using the experimental data and the COSMO-RS model and replaced in the process. As illustrated in Table S4, the relative deviation ( $\delta$ ) between the simulated value of the main process index for the extraction column and the actual data was less than 2.5%, indicating that the obtained binary interaction parameters using the experimental data and the COSMO-RS model at 313.15 K under a pressure of 101.3 kPa can be reliably used in designing and optimizing the extraction of aromatics using sulfolane.

## S6. The analysis of $\sigma$ -profiles.

In this section, the extraction of benzene and toluene using sulfolane is initially explored using the  $\sigma$ -profile [3-5], which can be used to reflect the intermolecular interactions. In the  $\sigma$ -profile, the shapes and positions of the different peaks indicate different properties. As shown in Figure S1, the shielding charge density was divided into three regions. The region in which  $\sigma < -0.0084 \text{ e}\text{\AA}^{-2}$  corresponds to the hydrogen bond donor (HBD) region; that is, when the molecule is in this region, it has the ability to provide electrons in the process of hydrogen bond formation, and the larger the peak and peak height area, the stronger the ability to provide electrons. When  $\sigma > +0.0084 \text{ e}\text{\AA}^{-2}$ , the molecule is in the hydrogen bond acceptor (HBA) region and has the ability to receive electrons during the formation of hydrogen bonds; the larger the peak height and peak area, the stronger the ability to receive electrons. When  $-0.0084 \text{ e}\text{\AA}^{-2} < \sigma < +0.0084 \text{ e}\text{\AA}^{-2}$ , the molecule is in the non-polar (non-polar) region; that is, the molecule neither provides nor receives electrons in this region.

As shown in Figure S1, the  $\sigma$ -profiles of benzene and toluene were mainly concentrated in the non-polar region. In the HBA region, the  $p(\sigma)$  values of benzene and toluene were less than 2.5, indicating that both had a weak ability to accept hydrogen bonds. In the HBA region, sulfolane had a higher  $p(\sigma)$  value, indicating a stronger ability to accept hydrogen bonds. In the HBD region, the  $p(\sigma)$  value of benzene and toluene were zero. During the extraction process, the HBA region of sulfolane did not overlap with the HBD regions of benzene and toluene. In contrast, in the HBD region, the smaller  $p(\sigma)$  value for sulfolane indicated hydrogen-bonding interactions with the HBA region of benzene and toluene. When  $\sigma = \pm 0.005 \text{ e}\text{\AA}^{-2}$ , the shape of the peaks of sulfolane was similar to that of benzene and toluene, and some peaks overlapped, which explain the higher solubility of sulfolane in benzene and toluene. The  $\sigma$ -profiles of alkanes are all in the non-polar region, indicating that those alkanes have no ability to form hydrogen bonds.

3. Diedenhofen, M.; Klamt, A. COSMO-RS as a tool for property prediction of IL mixtures—A review. *Fluid Phase Equilibria* **2010**, *294*, 31–38. <https://doi.org/10.1016/j.fluid.2010.02.002>.
4. Lemaoui, T.; Darwish, A.S.; Hammoudi, N.E.H.; Abu Hatab, F.; Attoui, A.; Alnashef, I.M.; Benguerba, Y. Prediction of electrical conductivity of deep eutectic solvents using COSMO-RS sigma profiles as molecular descriptors: A quantitative structure-property relationship study. *Industrial & Engineering Chemistry Research* **2020**, *59*, 13343–13354. <https://doi.org/10.1021/acs.iecr.0c02542>.
5. Wang, L.; Zhao, J.; Teng, J.; Dong, S.; Wang, Y.; Xiang, S.; Sun, X. Study on an energy-saving process for separation ethylene glycol mixture through heat-pump, heat-integration and ORC driven by waste-heat. *Energy* **2022**, *243*, 122985. <https://doi.org/10.1016/j.energy.2021.122985>.

## S7. The interaction analysis.

Table S6 shows the interaction energies of the eight complexes, where the values were corrected using the BSSE. Figure S2 shows different complex configurations with the lowest energies. As shown in Figure S2a, the distances of C1...H21, C4...H14, and O26...H9 are 2.84, 2.78, and 2.61 Å, respectively, indicating the formation of hydrogen bonding interactions between these atoms. As shown in Figure S2b, the distances of O6...H30, C17...H13, and C19...H13 are 2.43, 2.77, and 2.99 Å, respectively; thus, hydrogen bonding interactions are also formed between the O6...H30 and C17...H13 atoms, and C19...H13 forms van der Waals interactions. In addition, hydrogen bonding and van der Waals interactions are also present between the C...H and O...H atoms (Figure S2c-j). The  $|\Delta E_{\text{interaction}}|$  for the interplay of benzene and sulfolane and toluene and sulfolane were 28.74 kJ·mol<sup>-1</sup> and 35.73 kJ·mol<sup>-1</sup>, respectively, whereas  $|\Delta E_{\text{interaction}}|$  for the interactions between cyclopentane and sulfolane, n-pentane and sulfolane, cyclohexane and sulfolane, n-hexane and sulfolane, 3-methylpentane and sulfolane, and n-heptane and sulfolane were generally less than 28.74 kJ·mol<sup>-1</sup>, indicating that sulfolane is more selective for benzene and toluene than alkanes.

S8. The calculation details of the NRTL and UNIQUAC models.

The equation of the NRTL model is as follows:

$$\ln \gamma_i = \frac{\sum_{j=1}^n x_j \tau_{ji} G_{ji}}{\sum_{k=1}^n x_k G_{ki}} + \sum_{j=1}^n \frac{x_j G_{ij}}{\sum_{k=1}^n x_k G_{kj}} \left( \tau_{ij} - \frac{\sum_{m=1}^n x_m \tau_{mj} G_{mj}}{\sum_{k=1}^n x_k G_{kj}} \right)$$

where n is the number of components and  $\gamma_i$  is the activity coefficient of component i,

$$\tau_{ji} = \frac{g_{ji} - g_{ii}}{RT}, \quad \tau_{ij} = \frac{g_{ij} - g_{jj}}{RT}, \quad G_{ji} = \exp(-\alpha_{ji} \tau_{ji}), \quad G_{ij} = \exp(-\alpha_{ij} \tau_{ij}), \quad g_{ij} = g_{ji}. \text{ The } \tau_{ij}$$

and  $\tau_{ji}$  variables can be written as a function of temperature, as shown below:

$$\tau_{ij} = a_{ij} + \frac{b_{ij}}{T} + e_{ij} \ln T + f_{ij} T$$

Here,  $\alpha_{ij} = \alpha_{ji}$ . The equation of the UNIQUAC model is as follows:

$$\ln \gamma_i = \ln \frac{\Phi_i}{x_i} + \frac{z}{2} q_i \ln \frac{\theta_i}{\Phi_i} - q_i \ln \left( \sum_j \theta_j \tau_{ji} \right) - q_i \sum_j \frac{\theta_j \tau_{ij}}{t_j} + l_i + q_i' - \frac{\Phi_i}{x_i} \sum_j x_j l_j$$

$$\text{Here, } \Phi_i = \frac{r_i x_i}{\sum_k r_k x_k}, \quad \theta_i = \frac{q_i x_i}{\sum_k q_k x_k}, \quad \theta_i' = \frac{q_i' x_i}{\sum_k q_k' x_k}, \quad l_i = \frac{z}{2} (r_i - q_i) + 1 - r_i,$$

$$\tau_{ij} = \exp \left( -\frac{u_{ij} - u_{ji}}{RT} \right). \text{ and the } \tau_{ij} \text{ and } \tau_{ji} \text{ variables can be written as a function of temperature}$$

as well, as shown below:

$$\tau_{ij} = \exp \left( a_{ij} + \frac{b_{ij}}{T} + c_{ij} \ln T + d_{ij} T + \frac{d_{ij}}{T^2} \right)$$

Table S1. Chemical properties of materials.

Name	Formula	CAS No.	Mass fraction purity	Purification method	Supplier
Cyclopentane	C <sub>5</sub> H <sub>10</sub>	287-92-3	99% <sup>1</sup>	None	ARCOS
3-Methylpentane	C <sub>6</sub> H <sub>14</sub>	96-14-0	>99% <sup>1</sup>	None	ARCOS
Benzene	C <sub>6</sub> H <sub>6</sub>	71-43-2	>99.5% <sup>1</sup>	None	ARCOS
Toluene	C <sub>7</sub> H <sub>8</sub>	108-88-3	99.8% <sup>1</sup>	None	ARCOS
Sulfolane	C <sub>4</sub> H <sub>8</sub> O <sub>2</sub> S	126-33-0	>99% <sup>1</sup>	None	Sigma- Aldrich

<sup>1</sup> As stated by the supplier.

Table S2. The specific test conditions for Agilent GC7890A.

Project	Condition
Detector	Hydrogen flame ionization detector (FID)
Chromatographic column	SE-52 capillary column <sup>1</sup> , $\Phi$ 0.30 mm $\times$ 60 m
Injection volume	0.2 $\mu$ L
Sample chamber temperature	473.15 K
Detector temperature	523.15 K
Carrier gas (nitrogen) flow rate	0.6 ml $\cdot$ min <sup>-1</sup>
Hydrogen flow rate	30 ml $\cdot$ min <sup>-1</sup>
Air flow rate	300 ml $\cdot$ min <sup>-1</sup>

<sup>1</sup> Column stationary phase: 5% phenyl and 95% dimethyl polysiloxane. Physical properties of stationary phase: high column efficiency, solvent washout resistance, and good thermal stability, etc.

Table S3. The test results of gas chromatograph (FID) performance verification.

Performance index	Test result
Temperature accuracy of column chamber (0.50 %)	0.23
Programmed temperature repeatability ( $\leq 2$ %)	1.55
Baseline noise (30min, $\leq 1 \times 10^{-12}$ A)	$5.18 \times 10^{-14}$
Baseline drift ( $\leq 1 \times 10^{-11}$ A)	$3.10 \times 10^{-12}$
Limit of detection ( $N \leq 5 \times 10^{-11}$ g $\cdot$ s <sup>-1</sup> )	$2.57 \times 10^{-12}$
Quantitative repeatability ( $\leq 3$ %)	0.26
Qualitative repeatability ( $\leq 2$ %)	0.08
Linearity range ( $\geq 1 \times 10^6$ )	$3.48 \times 10^6$

Table S4. Liquid–liquid equilibrium data (molar fraction) for non-aromatics (1)–benzene (2)–sulfolane (3) ternary systems at 293.15 K, or 313.15 K under 101.3 kPa using the COSMO-RS model.

<i>T/K</i>	Sulfolane rich phase			Sulfolane poor phase			<i>D</i>	<i>S</i>
	$x_1^I$	$x_2^I$	$x_3^I$	$x_1^{II}$	$x_2^{II}$	$x_3^{II}$		
<b>Cyclopentane (1)–Benzene (2)–Sulfolane (3)</b>								
313.15	0.0591	0.0000	0.9409	0.9980	0.0000	0.0020	–	–
	0.0655	0.0619	0.8726	0.8711	0.1229	0.0060	0.3728	6.7047
	0.0701	0.1043	0.8256	0.7846	0.2043	0.0111	0.3818	5.7099
	0.0763	0.1582	0.7655	0.6765	0.3021	0.0214	0.3985	4.6420
	0.0800	0.1892	0.7309	0.6173	0.3536	0.0291	0.4118	4.1294
	0.0844	0.2254	0.6903	0.5523	0.4081	0.0396	0.4313	3.6162
	0.0884	0.2578	0.6539	0.4987	0.4511	0.0503	0.4526	3.2245
<b><i>n</i>-Pentane (1)–Benzene (2)–Sulfolane (3)</b>								
298.15	0.0314	0.0000	0.9686	0.9983	0.0000	0.0017	–	–
	0.0350	0.0512	0.9138	0.8893	0.1067	0.0040	0.3010	12.2011
	0.0391	0.1024	0.8586	0.7823	0.2092	0.0085	0.3167	9.8021
	0.0449	0.1679	0.7872	0.6497	0.3316	0.0187	0.3423	7.3365
	0.0494	0.2151	0.7355	0.5605	0.4101	0.0295	0.3666	5.9515
	0.0500	0.2211	0.7289	0.5497	0.4193	0.0310	0.3701	5.7972
	0.0581	0.2974	0.6445	0.4249	0.5206	0.0545	0.4241	4.1800
	0.0631	0.3410	0.5959	0.3643	0.5647	0.0710	0.4636	3.4873
	0.0723	0.4117	0.5160	0.2817	0.6152	0.1031	0.5438	2.6080
<b>Cyclohexane (1)–Benzene (2)–Sulfolane (3)</b>								
298.15	0.0267	0.0162	0.9571	0.9636	0.0348	0.0016	0.3296	16.7585
	0.0297	0.0644	0.9059	0.8593	0.1372	0.0035	0.3366	13.6004
	0.0305	0.0780	0.8915	0.8303	0.1654	0.0043	0.3391	12.8141
	0.0326	0.1079	0.8596	0.7667	0.2265	0.0068	0.3453	11.2106
	0.0346	0.1371	0.8283	0.7053	0.2845	0.0102	0.3525	9.8090
	0.0365	0.1615	0.8021	0.6550	0.3312	0.0139	0.3595	8.7584
	0.0387	0.1908	0.7705	0.5958	0.3847	0.0195	0.3695	7.6308
	0.0408	0.2174	0.7417	0.5440	0.4303	0.0257	0.3803	6.7301
	0.0435	0.2505	0.7060	0.4833	0.4819	0.0348	0.3967	5.7685
	0.0459	0.2780	0.6761	0.4363	0.5203	0.0434	0.4130	5.0832
<b><i>n</i>-Hexane (1)–Benzene (2)–Sulfolane (3)</b>								
298.15	0.0141	0.0406	0.9453	0.9063	0.0914	0.0023	0.3218	28.5377

Table S4 (continued).

	0.0176	0.1211	0.8614	0.7303	0.2626	0.0071	0.3393	19.1708
	0.0209	0.1854	0.7937	0.5978	0.3868	0.0154	0.3586	13.7270
	0.0230	0.2221	0.7549	0.5268	0.4508	0.0224	0.3727	11.2890
	0.0254	0.2609	0.7138	0.4565	0.5118	0.0317	0.3910	9.1670
	0.0278	0.2978	0.6744	0.3954	0.5623	0.0423	0.4122	7.5261
	0.0311	0.3440	0.6249	0.3277	0.6146	0.0578	0.4448	5.8995
	0.0352	0.3978	0.5670	0.2608	0.6600	0.0792	0.4924	4.4602
	0.0358	0.4052	0.5590	0.2526	0.6650	0.0824	0.4998	4.2933
	0.0367	0.4156	0.5477	0.2414	0.6715	0.0871	0.5106	4.0691
	<b>3-Methylpentane (1)–Benzene (2)–Sulfolane (3)</b>							
313.15	0.0210	0.0000	0.9790	0.9980	0.0000	0.0020	–	–
	0.0241	0.0563	0.9197	0.8727	0.1229	0.0044	0.3339	16.6094
	0.0274	0.1099	0.8627	0.7585	0.2327	0.0088	0.3484	13.0511
	0.0310	0.1600	0.8090	0.6570	0.3274	0.0156	0.3653	10.3452
	0.0344	0.2027	0.7629	0.5752	0.4010	0.0238	0.3830	8.4511
	0.0437	0.3054	0.6509	0.4039	0.5433	0.0528	0.4439	5.1963
	0.0482	0.3490	0.6028	0.3441	0.5869	0.0690	0.4796	4.2446

Table S5. Liquid–liquid equilibrium data (molar fraction) for non-aromatics (1)–toluene (2)–sulfolane (3) ternary systems at 293.15 K, or 313.15 K under 101.3 kPa using the COSMO-RS model.

<i>T</i> /K	Sulfolane rich phase			Sulfolane poor phase			<i>D</i>	<i>S</i>
	$x_1^I$	$x_2^I$	$x_3^I$	$x_1^{II}$	$x_2^{II}$	$x_3^{II}$		
<b>Cyclopentane (1)–Toluene (2)–Sulfolane (3)</b>								
313.15	0.0591	0.0000	0.9409	0.9980	0.0000	0.0020	–	–
	0.0605	0.0321	0.9075	0.8835	0.1114	0.0052	0.1804	4.2070
	0.0620	0.0957	0.8423	0.6650	0.3156	0.0195	0.2069	3.2541
	0.0621	0.1226	0.8153	0.5825	0.3888	0.0287	0.2223	2.9567
	0.0621	0.1346	0.8033	0.5485	0.4183	0.0332	0.2300	2.8413
	0.0619	0.1646	0.7735	0.4713	0.4832	0.0455	0.2514	2.5911
	0.0615	0.2013	0.7372	0.3914	0.5468	0.0618	0.2816	2.3432
<b><i>n</i>-Pentane (1)–Toluene (2)–Sulfolane (3)</b>								
298.15	0.0253	0.0000	0.9747	0.9988	0.0000	0.0012	–	–
	0.0263	0.0304	0.9433	0.8775	0.1195	0.0030	0.1610	8.5059
	0.0270	0.0575	0.9155	0.7702	0.2236	0.0062	0.1687	7.3445
	0.0276	0.0901	0.8823	0.6459	0.3414	0.0127	0.1806	6.1773
	0.0279	0.1209	0.8512	0.5380	0.4403	0.0217	0.1950	5.2869
	0.0280	0.1372	0.8348	0.4858	0.4867	0.0275	0.2040	4.8888
	0.0280	0.1414	0.8306	0.4731	0.4978	0.0291	0.2064	4.7946
	0.0278	0.1925	0.7797	0.3392	0.6101	0.0507	0.2413	3.8494
	0.0274	0.2220	0.7506	0.2790	0.6565	0.0646	0.2652	3.4395
<b>Cyclohexane (1)–Toluene (2)–Sulfolane (3)</b>								
298.15	0.0265	0.0194	0.9541	0.9214	0.0764	0.0022	0.1815	8.8361
	0.0267	0.0269	0.9464	0.8916	0.1057	0.0027	0.1826	8.4867
	0.0271	0.0388	0.9341	0.8443	0.1520	0.0037	0.1847	7.9612
	0.0276	0.0585	0.9140	0.7670	0.2268	0.0062	0.1889	7.1679
	0.0279	0.0738	0.8982	0.7079	0.2833	0.0088	0.1930	6.6086
	0.0283	0.0938	0.8779	0.6337	0.3529	0.0133	0.1994	5.9559
	0.0285	0.1111	0.8604	0.5725	0.4093	0.0182	0.2061	5.4536
	0.0286	0.1290	0.8424	0.5133	0.4625	0.0242	0.2141	4.9965
	0.0287	0.1469	0.8244	0.4584	0.5106	0.0310	0.2234	4.5936
	0.0285	0.1920	0.7795	0.3416	0.6077	0.0506	0.2522	3.7861
<b><i>n</i>-Hexane (1)–Toluene (2)–Sulfolane (3)</b>								
298.15	0.0137	0.0433	0.9429	0.8186	0.1775	0.0039	0.1799	14.5554

Table S5 (continued).

	0.0145	0.0778	0.9076	0.6822	0.3094	0.0084	0.1890	11.8216
	0.0150	0.1020	0.8830	0.5926	0.3939	0.0135	0.1972	10.2259
	0.0153	0.1188	0.8659	0.5339	0.4481	0.0179	0.2039	9.2519
	0.0157	0.1431	0.8412	0.4559	0.5183	0.0257	0.2152	8.0345
	0.0159	0.1668	0.8173	0.3883	0.5770	0.0347	0.2283	7.0377
	0.0162	0.2067	0.7770	0.2936	0.6544	0.0520	0.2548	5.7067
	0.0163	0.2139	0.7698	0.2789	0.6657	0.0554	0.2603	5.5050
	0.0163	0.2211	0.7626	0.2651	0.6761	0.0588	0.2658	5.3156
	<b>3-Methylpentane (1)–Toluene (2)–Sulfolane (3)</b>							
313.15	0.0210	0.0000	0.9790	0.9980	0.0000	0.0020	–	–
	0.0229	0.0537	0.9234	0.7896	0.2035	0.0069	0.1960	9.0823
	0.0237	0.0777	0.8986	0.7024	0.2866	0.0110	0.2041	8.0193
	0.0250	0.1185	0.8565	0.5666	0.4121	0.0213	0.2214	6.5169
	0.0256	0.1418	0.8325	0.4974	0.4735	0.0290	0.2336	5.8133
	0.0268	0.1927	0.7804	0.3713	0.5795	0.0493	0.2667	4.6060
	0.0280	0.2580	0.7140	0.2556	0.6648	0.0796	0.3217	3.5381
	0.0283	0.2714	0.7004	0.2371	0.6767	0.0862	0.3346	3.3654
	<b><i>n</i>-Heptane (1)–Toluene (2)–Sulfolane (3)</b>							
298.15	0.0069	0.0219	0.9712	0.9035	0.0943	0.0022	0.1933	30.2432
	0.0073	0.0425	0.9502	0.8166	0.1799	0.0035	0.1966	26.4006
	0.0078	0.0672	0.9251	0.7174	0.2767	0.0060	0.2015	22.4329
	0.0082	0.0888	0.9030	0.6348	0.3561	0.0091	0.2069	19.4236
	0.0085	0.1104	0.8810	0.5572	0.4294	0.0134	0.2133	16.8109
	0.0089	0.1324	0.8587	0.4839	0.4971	0.0190	0.2212	14.5120
	0.0092	0.1550	0.8358	0.4153	0.5586	0.0261	0.2308	12.4958
	0.0095	0.1773	0.8131	0.3547	0.6109	0.0344	0.2421	10.8053
	0.0099	0.2102	0.7799	0.2789	0.6728	0.0483	0.2622	8.7909
	0.0102	0.2416	0.7482	0.2206	0.7163	0.0631	0.2851	7.2945

Table S6. The *RMSD* values of the COSMO-RS model at 293.15 K, or 313.15 K under 101.3 kPa.

<b>T/K</b>	<b>System</b>	<b>RMSD value</b>
313.15	Cyclopentane (1)–Benzene (2)–Sulfolane (3)	0.0898
313.15	Cyclopentane (1)–Toluene (2)–Sulfolane (3)	0.0687
293.15	<i>n</i> -Pentane (1)–Benzene (2)–Sulfolane (3)	0.0449
293.15	<i>n</i> -Pentane (1)–Toluene (2)–Sulfolane (3)	0.0661
293.15	Cyclohexane (1)–Benzene (2)–Sulfolane (3)	0.0449
293.15	Cyclohexane (1)–Toluene (2)–Sulfolane (3)	0.0334
293.15	<i>n</i> -Hexane (1)–Benzene (2)–Sulfolane (3)	0.0882
293.15	<i>n</i> -Hexane (1)–Toluene (2)–Sulfolane (3)	0.0782
313.15	3-Methylpentane (1)–Benzene (2)–Sulfolane (3)	0.0492
313.15	3-Methylpentane (1)–Toluene (2)–Sulfolane (3)	0.0727
293.15	<i>n</i> -Heptane (1)–Toluene (2)–Sulfolane (3)	0.0704

Table S7. Comparison of the main process indexes of C01.

	Components	$x^{\text{act}}/\text{wt}\%$	$x^{\text{UNIFAC}}/\text{wt}\%$	$\Delta$	$\delta\%$	$x^{\text{experiment}}/\text{wt}\%$	$\Delta$	$\delta\%$	$x^{\text{sim}}/\text{wt}\%$	$\Delta$	$\delta\%$
Column top	<i>n</i> -Pentane	9.72	9.72	0.00	0.00	9.74	0.02	0.21	9.74	0.02	0.21
	Cyclopentane	1.68	1.69	0.01	0.60	1.69	0.01	0.60	1.69	0.01	0.60
	<i>n</i> -Hexane	20.26	20.47	0.21	1.04	20.51	0.25	1.23	20.51	0.25	1.23
	Cyclohexane	1.22	1.23	0.01	0.82	1.23	0.01	0.82	1.23	0.01	0.82
	3-Methylpentane	26.07	26.02	-0.05	0.19	26.03	-0.04	0.15	26.07	0.00	0.00
	<i>n</i> -Heptane	12.51	12.79	0.28	2.24	12.82	0.31	2.48	12.82	0.31	2.48
Column bottom	Benzene	9.51	8.82	-0.69	7.26	9.23	-0.28	2.94	9.32	-0.19	2.00
	Toluene	16.49	15.97	-0.52	3.15	16.14	-0.35	2.12	16.18	-0.31	1.88
	Sulfolane	70.49	70.48	-0.01	0.01	70.48	-0.01	0.01	70.49	0.00	0.00

Here,  $x^{\text{act}}$  denotes the actual industrial data,  $x^{\text{UNIFAC}}$  denotes the simulated values using the UNIFAC model,  $x^{\text{experiment}}$  denotes the simulated values using experimental data, and  $x^{\text{sim}}$  denotes the simulated values using the COSMO-RS model. The  $\Delta$  and  $\delta$  calculation formulas are given in Manuscript 4.4.

Table S8. Interaction energy of eight complexes corrected using BSSE.

Complex	$E_{BSSE}(\text{kJ}\cdot\text{mol}^{-1})$	$\Delta E_{\text{interaction}}(\text{kJ}\cdot\text{mol}^{-1})$
Benzene–Sulfolane	4.16	-28.74
Toluene–Sulfolane	5.33	-35.73
Cyclopentane–Sulfolane	4.41	-20.25
<i>n</i> -Pentane–Sulfolane	4.19	-20.67
Cyclohexane–Sulfolane	3.22	-20.54
<i>n</i> -Hexane–Sulfolane	4.24	-23.18
3-Methylpentane–Sulfolane	4.08	-22.68
<i>n</i> -Heptane–Sulfolane	4.26	-22.89

Table S9. The RMSD values of the NRTL and UNIQUAC models.

T/K	System	RMSD value	
		NRTL	UNIQUAC
313.15	Cyclopentane (1)–Benzene (2)–Sulfolane (3)	0.0007	0.0019
313.15	Cyclopentane (1)–Toluene (2)–Sulfolane (3)	0.0013	0.0007
293.15	<i>n</i> -Pentane (1)–Benzene (2)–Sulfolane (3)	0.0018	0.0025
293.15	<i>n</i> -Pentane (1)–Toluene (2)–Sulfolane (3)	0.0103	0.0013
293.15	Cyclohexane (1)–Benzene (2)–Sulfolane (3)	0.0008	0.0016
293.15	Cyclohexane (1)–Toluene (2)–Sulfolane (3)	0.0182	0.0180
293.15	<i>n</i> -Hexane (1)–Benzene (2)–Sulfolane (3)	0.0052	0.0022
293.15	<i>n</i> -Hexane (1)–Toluene (2)–Sulfolane (3)	0.0043	0.0017
313.15	3-Methylpentane (1)–Benzene (2)–Sulfolane (3)	0.0021	0.0015
313.15	3-Methylpentane (1)–Toluene (2)–Sulfolane (3)	0.0023	0.0022
293.15	<i>n</i> -Heptane (1)–Toluene (2)–Sulfolane (3)	0.0010	0.0025

Table S10. The binary interaction parameters for ternary mixtures using the UNQUAC model.

<b>Ternary blends</b>	<b><i>i-j</i></b>	<b><i>a<sub>ij</sub></i></b>	<b><i>a<sub>ji</sub></i></b>	<b><i>b<sub>ij</sub></i></b>	<b><i>b<sub>ji</sub></i></b>	<b><i>RMSD</i></b>
Cyclopentane (1)–Benzene (2)–Sulfolane (3)	1–2	0.8117	-0.7645	-209.6848	69.0400	0.0019
	1–3	0.0000	0.0000	-527.9870	-96.6703	
	2–3	0.0000	0.0000	-58.7940	-160.1311	
Cyclopentane (1)–Toluene (2)–Sulfolane (3)	1–2	0.0000	0.0000	-306.6952	206.2113	0.0007
	1–3	0.0000	0.0000	-532.7111	-102.1904	
	2–3	-1.1594	0.6053	163.9709	-208.8493	
<i>n</i> -Pentane (1)–Benzene (2)–Sulfolane (3)	1–2	0.0000	0.0000	-315.7150	204.2730	0.0025
	1–3	7.6564	-2.2062	-2799.4711	579.0377	
	2–3	0.0000	0.0000	-142.8626	-19.0645	
<i>n</i> -Pentane (1)–Toluene (2)–Sulfolane (3)	1–2	0.0000	0.0000	-296.5301	198.9147	0.0013
	1–3	0.0000	0.0000	-559.1037	-87.8081	
	2–3	0.0000	0.0000	-191.8146	-25.2332	
Cyclohexane (1)–Benzene (2)–Sulfolane (3)	1–2	0.0000	0.0000	-239.1089	153.2099	0.0016
	1–3	1.4214	-0.3091	-970.6103	-7.7795	
	2–3	0.0000	0.0000	-112.0568	-47.9761	
Cyclohexane (1)–Toluene (2)–Sulfolane (3)	1–2	0.0000	0.0000	133.8295	-245.0781	0.0180
	1–3	0.3808	0.4604	-666.7487	-230.7804	
	2–3	0.0000	0.0000	-145.7145	-75.0009	
<i>n</i> -Hexane (1)–Benzene (2)–Sulfolane (3)	1–2	0.0000	0.0000	-267.5298	171.3638	0.0022
	1–3	0.0000	0.0000	-544.0078	-92.8109	
	2–3	0.0000	0.0000	-126.8512	-40.1255	
<i>n</i> -Hexane (1)–Toluene (2)–Sulfolane (3)	1–2	0.0000	0.0000	-315.4590	204.2369	0.0017
	1–3	0.0000	0.0000	-563.0780	-92.7991	
	2–3	0.0000	0.0000	-194.1372	-22.6599	
3-Methylhexane (1)–Benzene (2)–Sulfolane (3)	1–2	0.0000	0.0000	-305.2496	199.3378	0.0015
	1–3	0.0000	0.0000	-558.7968	-61.5939	
	2–3	0.0000	0.0000	-112.2377	-45.9939	
3-Methylpentane (1)–Toluene (2)–Sulfolane (3)	1–2	0.0000	0.0000	-126.6496	77.9116	0.0022
	1–3	0.0000	0.0000	-512.5936	-12.6276	
	2–3	0.0000	0.0000	-161.8310	-7.8291	
<i>n</i> -Heptane (1)–Toluene (2)–Sulfolane (3)	1–2	0.0000	0.0000	-263.3599	181.3304	0.0025
	1–3	0.0000	0.0000	-552.0777	-94.1506	
	2–3	-1.1594	0.6053	159.1383	-205.9555	

Table S11. The feed compositions (stream 2) of the extraction device.

Name	Formula	CAS No.	Mass fraction (%)
<i>n</i> -Butane	C <sub>4</sub> H <sub>10</sub>	106-97-8	0.010
<i>n</i> -Pentane	C <sub>5</sub> H <sub>12</sub>	109-66-0	3.800
1-Pentene	C <sub>5</sub> H <sub>10</sub>	109-67-1	0.370
Cyclopentane	C <sub>5</sub> H <sub>10</sub>	287-92-3	0.661
<i>n</i> -Hexane	C <sub>6</sub> H <sub>14</sub>	110-54-3	8.000
3-Methylpentane	C <sub>6</sub> H <sub>14</sub>	96-14-0	10.170
1-Hexene	C <sub>6</sub> H <sub>12</sub>	592-41-6	0.604
Cyclohexane	C <sub>6</sub> H <sub>12</sub>	110-82-7	0.481
Benzene	C <sub>6</sub> H <sub>6</sub>	71-43-2	18.190
<i>n</i> -Heptane	C <sub>7</sub> H <sub>16</sub>	142-82-5	5.000
2-Methylhexane	C <sub>7</sub> H <sub>16</sub>	591-76-4	6.350
1-Heptene	C <sub>7</sub> H <sub>14</sub>	592-76-7	0.746
Cycloheptane	C <sub>7</sub> H <sub>14</sub>	291-64-5	0.519
Toluene	C <sub>7</sub> H <sub>8</sub>	108-88-3	42.660
<i>n</i> -Octane	C <sub>8</sub> H <sub>18</sub>	111-65-9	1.804
1-Octene	C <sub>8</sub> H <sub>16</sub>	111-66-0	0.009
Cyclooctane	C <sub>8</sub> H <sub>16</sub>	292-64-8	0.236
<i>p</i> -Xylene	C <sub>8</sub> H <sub>10</sub>	106-42-3	0.360
Water	H <sub>2</sub> O	7732-18-5	0.030

Table S12. The key component settings of C01.

Name	Key components
1st liquid phase	<i>n</i> -Pentane
	Cyclopentane
	<i>n</i> -Hexane
	Cyclohexane
	3-Methylpentane
2nd liquid phase	<i>n</i> -Heptane
	Benzene
	Toluene
	Sulfolane

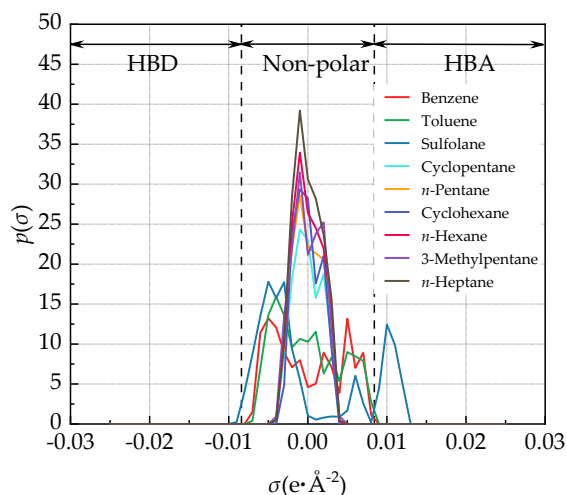


Figure S1. The  $\sigma$ -profiles of the nine substances in this study. The vertical dashed lines ( $\sigma = \pm 0.0084 \text{ e}\cdot\text{\AA}^{-2}$ ) indicate the threshold of hydrogen bonding interactions.

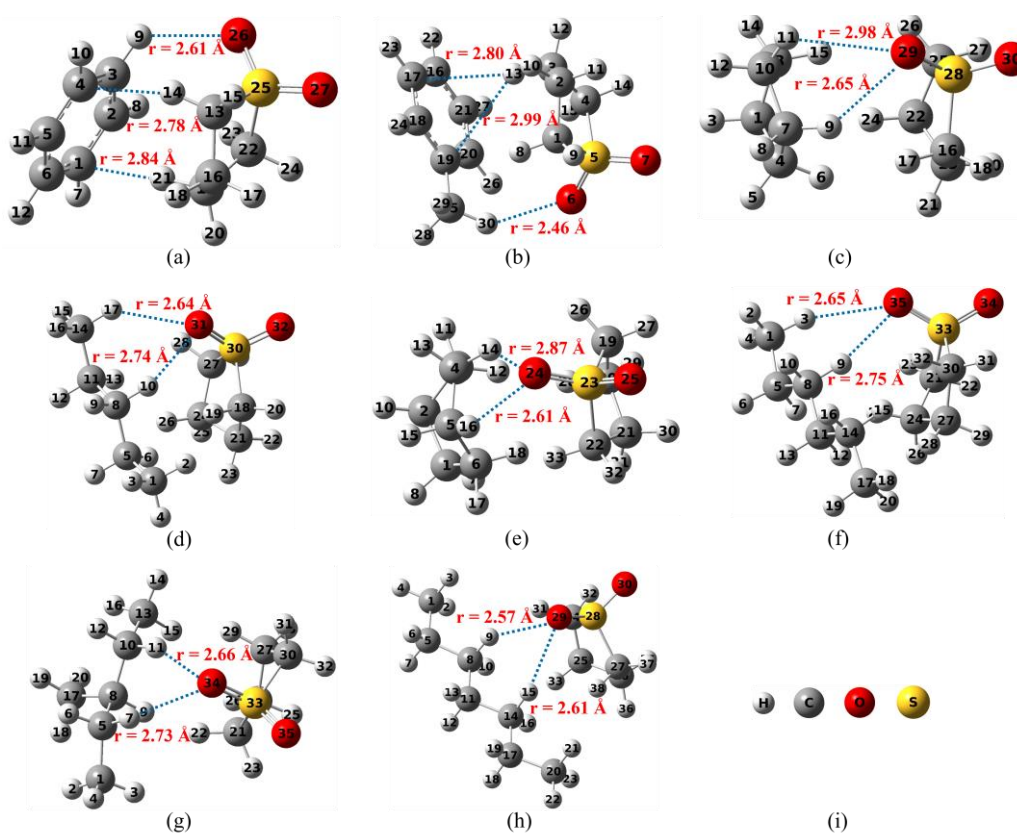


Figure S2. The complex configurations with the lowest energies. (a) Benzene–Sulfolane, (b) Toluene–Sulfolane, (c) Cyclopentane–Sulfolane, (d) *n*-Pentane–Sulfolane, (e) Cyclohexane–Sulfolane, (f) *n*-Hexane–Sulfolane, (g) 3-Methylpentane–Sulfolane, (h) *n*-Heptane–Sulfolane, (i) The color instructions of different elements. The dashed lines indicate possible interactions, the Bondi van der Waals radii used for the elemental radii, and the interatomic distances in angstroms.

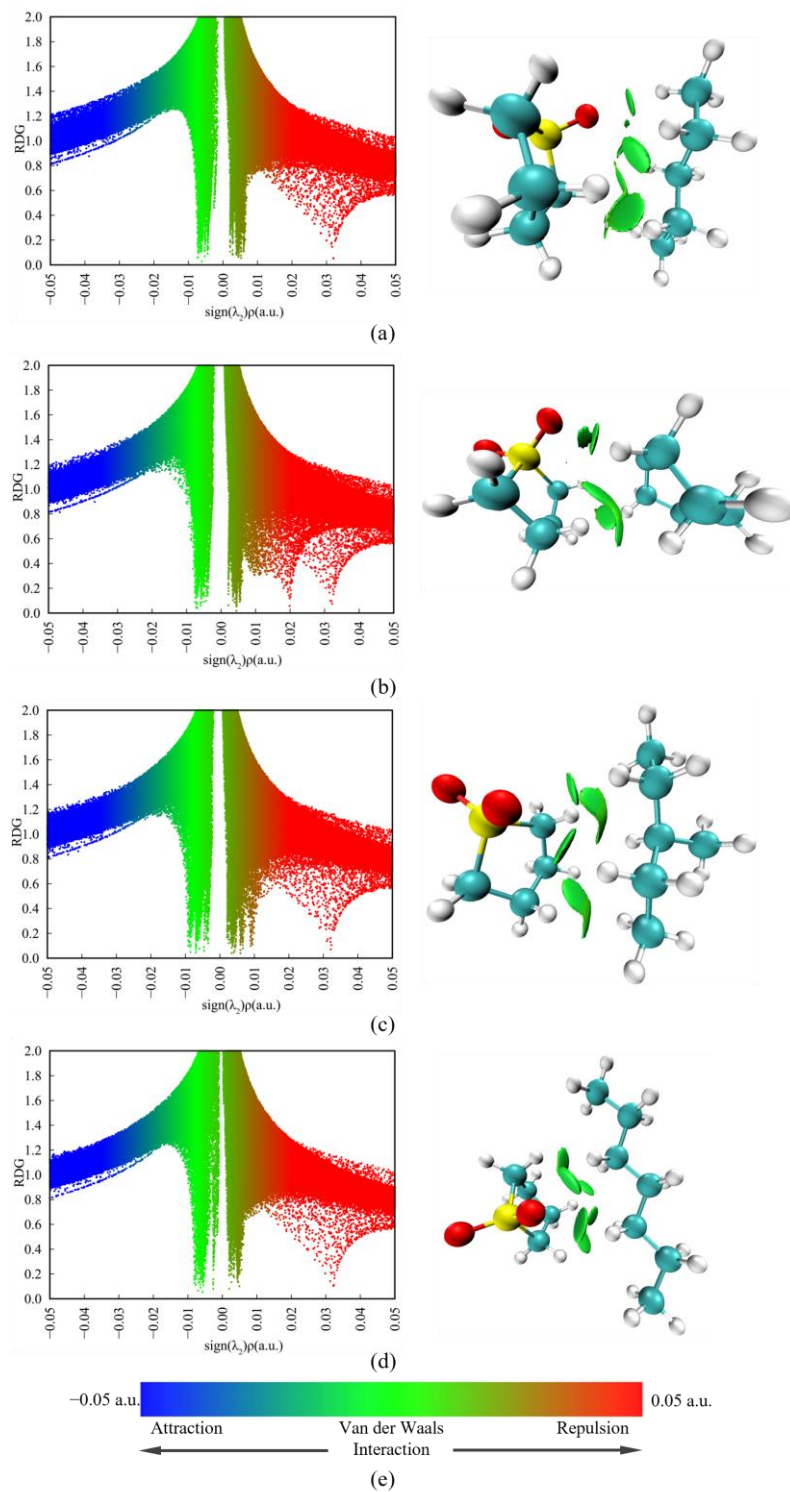


Figure S3. The RDG (left) and IGMH (right) of different complexes. (a) Sulfolane-*n*-Pentane; (b) Sulfolane-Cyclohexane; (c) Sulfolane-3-Methylpentane; (d) Sulfolane-*n*-Heptane; (e) The colors represented by the different  $\text{sign}(\lambda_2)\rho$ (a.u.) values and the types of their corresponding interactions. (IGMH isovalue = 0.006).